Mechanical and electrical properties of the Bi-Ge-Sn alloys

Aleksandar Djordjevic[1], Dusko Minic[1], Milena Premovic[1*], Milan Kolarevic[2], Milan Milosavljevic[1]

[1]*University of Priština in Kosovska Mitrovica, Faculty of Technical Science, Department of Technological engineering Kneza Milosa 7, 38220 Kos. Mitrovica, Serbia*

[2]*University of Kragujevac, Faculty of Mechanical Engineering, Kraljevo, Serbia*

Mechanical and electrical properties of the ternary Bi-Ge-Sn alloys were investigated in this study. Calculation of isothermal section at 200, 300 and 25 ºC was carried out by using optimized thermodynamic parameters for the constitutive binary systems. Microstructures of alloys were observed by using optical microscopy and scanning electron microscopy (SEM). Phases in microstructures have been detected by x-ray diffraction (XRD) analysis and compositions of the phasis by energy dispersive spectrometry (EDS). ANOVA analysis and using obtained results an appropriate mathematical model is proposed for every composition of alloys. The Brinell hardness and electrical conductivity of selected alloys were measured and obtained results were analyzed with respect to their overall compositions and phase constituents. Based on all the obtained experimental and calculated results, it was concluded that a general good agreement was obtained between them.

Keywords: Ternary Bi-Ge-Sn system, Microstructures, Hardness properties, Electrical properties

1. INTRODUCTION

As the properties of the material can be changed with the addition of other elements, the testing of other alloys is always current, in a way to obtain alloys with new properties. Due to the technical importance of germanium-based systems, our group has previously tested germanium-based systems [1-3]. Experimental examination and thermodynamic description of the ternary Bi-Ge-Sn system have been investigated by Aleksandar et al. [4]. Electrical and mechanical properties of ternary Bi-Ge-Sn system have not been investigated before. Germanium-based alloys are mainly used as memory materials [5-8]. Because of all that, in this study is shown experimental investigation of electrical and mechanical properties of the ternary Bi-Ge-Sn alloys at room temperature (≈25 °C), as well as isothermal sections on 200 and 300 °C. Thermodynamic data proposed by Aleksandar et al. [4] has been used in our study for the calculation of selected isothermal sections. Alloys of the tested ternary system tested with Brinell hardness test and test for electrical conductivity. Too, have been investigated phase equilibria of the isothermal sections at 200, 300 and 25 °C using scanning electron microscopy (SEM) with energy dispersive spectrometry (EDS) and x-ray diffraction (XRD). The results obtained in this paper were intended to provide a better insight into the properties of the test alloys.

2. MATERIALS AND METHODS

All tested samples (ternary and binary) with total masses of about 5 g were prepared from elements high purity (99.999 at. %) Bi, Ge, and Sn. Samples were melted in an induction furnace under high purity argon atmosphere and slowly cooled. The average weight loss of the samples during induction melting was about 1 mass %. Samples for investigation of isothermal sections at 200 °C and 300 °C, were sealed in evacuated quartz tubes and then heated to the appropriate temperatures. Then they were extinguished in the water and ice mixture to preserve desired equilibrium at appropriate temperatures (200 and 300 °C). Prepared samples in this way were examined SEM-EDS and XRD analysis. Samples cooled to room temperature were tested Brinell hardness and electrical conductivity.

The compositions of samples and coexisting phases were determined by using JEOL JSM-6460 scanning electron microscope with energy dispersive spectroscopy (EDS) (Oxford Instruments X-act). Powder XRD data for phase identification of samples were recorded on a D2 PHASER (Bruker, Karlsruhe, Germany) powder diffractometer equipped with a dynamic scintillation detector and ceramic X-ray Cu tube (KFL-Cu-2K) in a 2θ range from 10° to 75° with a step size of 0.02°. The patterns were analyzed using the Topas 4.2 software, ICDD databases PDF2. Microstructures of the samples were recorded on a light microscopy using (LOM) OLYMPUS GX41 inverted metallographic microscope. Hardnesses of the samples were measured using Brinell hardness tester INNOVATEST, model NEXUS 3001. Electrical conductivity measurements were carried out using Foerster SIGMATEST 2.069 eddy current instrument.

3. RESULTS AND DISCUSSION

Constitutive binary systems of the ternary Bi-Ge-Sn system were extensively studied in the past. Reliable thermodynamic datasets for these binary systems are available in literature [9-11]. Based on the literature information for binary sub-systems considered phase, their crystallographic data and database names for the solid phases are summarized in Table 1.

*Corresponding author: M. Premovic, milena.premovic@pr.ac.rs

Table 1: Considered phase, their crystallographic data and database names for the solid phases of the ternary Bi-Ge-Sn system

Thermodynamic database name	Common name	Space group symbol	Struktural designation	Pearson's symbol
LIQUID	Liquid	-	-	-
RHOMBO_A7	(Bi)	$R\bar{3}mH$	*A7*	*hR2*
DIAMOND_A4	(Ge)	$Fm\bar{3}m$	*A4*	*cF8*
DIAMOND_A4	(αSn)	$Fd\bar{3}m$	*A4*	*cF8*
BCT_A5	(βSn)	$I4_1/amd$	*A5*	*tI4*

In ternary Bi-Ge-Sn system, should appears liquid phase and four solid solution phases: (Bi), (Ge), (αSn) and (βSn).

3.1. Izothermal section at 200 °C.

For investigation of the phase equilibria at 200 °C, five samples were analyzed by SEM-EDS and XRD methods. Experimental results are summarized in Table 2.

Table 2: Combined results of SEM-EDS and XRD analyzes of the selected Bi-Ge-Sn alloys annealed at T=200 °C

N.	Composition of samples (at. %)	Determined phases		Compositions of phases (at. %)			Lattice parameters (Å)	
		EDS	XRD	Bi	Ge	Sn	*a=b*	*c*
1.	10.90 Bi 55.27 Ge 33.83 Sn	L (Ge)	 (Ge)	27.01±0.7 0.33±0.4	1.82±0.2 98.87±0.1	71.17±0.4 0.80±0.7	5.6545±0.0002	
2.	22.28 Bi 19.14 Ge 58.58 Sn	L (Ge)	 (Ge)	30.21±0.6 0.65±0.7	2.63±0.5 99.12±0.4	67.16±0.1 0.23±0.2	5.6589±0.0007	
3.	33.97 Bi 33.67 Ge 32.36 Sn	L (Ge)	 (Ge)	27.02±0.3 0.82±0.7	3.03±0.6 98.99±0.1	69.95±0.7 0.19±0.9	5.6536±0.0004	
4.	45.96 Bi 44.53 Ge 9.51 Sn	L (Ge) (Bi)	 (Ge) (Bi)	10.87±0.7 0.57±0.7 99.12±0.7	5.01±0.4 98.25±0.8 0.18±0.9	84.12±0.8 1.18±0.7 0.70±0.2	 5.6512±0.0006 4.5367±0.0004	 11.8124±0.0006
5.	63.79 Bi 13.61 Ge 22.60 Sn	L (Ge) (Bi)	 (Ge) (Bi)	7.53±0.9 1.07±0.2 98.76±0.1	5.27±0.7 98.12±0.7 0.62±0.8	87.20±0.8 0.81±0.1 0.62±0.9	 5.6578±0.0005 4.5398±0.0006	 11.8179±0.0003

As can be seen from the presented EDS and XRD results, the all studied alloy samples have the same L and (Ge) solid solution phase in microstructure. In addition to the liquid phase and (Ge) solid solution phase, in the samples 4 and 5 occur an (Bi) solid solution phase. The EDS results show that (Ge) solid solution phase is rich with germanium with neglected solubility of other two elements. (Bi) solid solution phase is rich with bismuth and with neglected solubility of germanium and tin. Liquid phase is rich with Bi and Sn.

SEM micrograph of one sample annealed at 200 °C is presented in Figure 1 as an illustration.

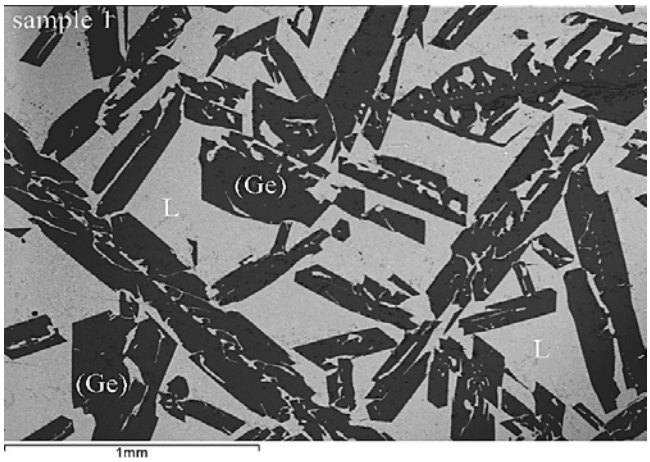

Figure 1: SEM micrographs of the sample 1 annealed at 200 ºC

On the given micrograph, (Ge) solid solution phase appears as a dark phase and L phase as a light phase.

Since the samples were annealed at 200 °C, compositions of the phases determined by EDS analysis were compared with the calculated isothermal section at 200 °C. Figure 2 shows comparison of the EDS results (Table 2) and the calculated isothermal section at 200 °C.

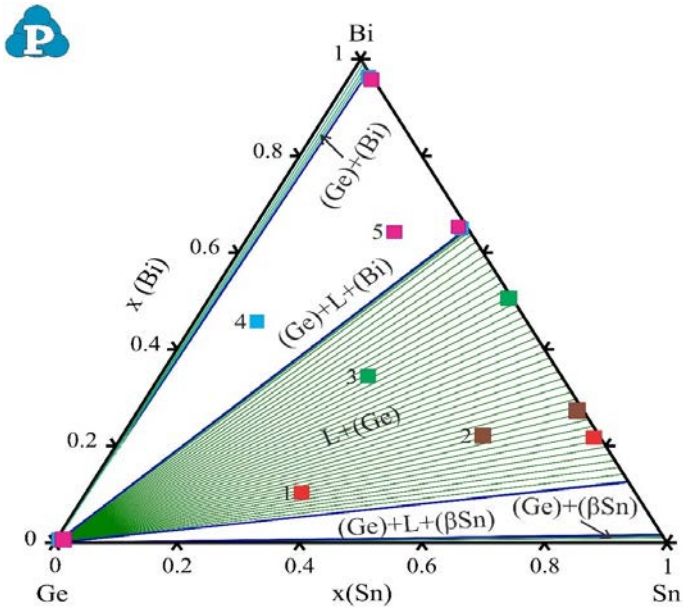

Figure 2: Calculated isothermal section at 200 °C compared with EDS results given in Table 2

From Figure 2 it can be seen that the calculated isothermal section has five phase regions. Three of them are L+(Ge), (Ge)+(βSn) and (Ge)+(Bi) two-phase regions, two are (Ge)+L+(Bi) and (Ge)+L+(βSn) three-phase regions. Two of the three phase regions have been experimentally proven. Tested alloy samples 1, 2 and 3 belong to L+(Ge) two-phase region. Samples 4 and 5 belong (Ge)+L+(Bi) three-phase region.

3.2. Isothermal section at 300 °C

As a next step, five alloys annealed at 300 °C were used for checking phase equilibria at 300 °C. Results of SEM-EDS and XRD analysis for the alloys annealed at 300 °C are summarized in Table 3.

Table 3: Combined results of SEM-EDS and XRD analyzes of the selected Bi-Ge-Sn alloys annealed at T=300 °C

N.	Composition of samples (at. %)	Determined phases		Compositions of phases (at. %)			Lattice parameters (Å)
		EDS	XRD	Bi	Ge	Sn	*a=b=c*
1.	13.03 Bi 22.91 Ge 64.06 Sn	L (Ge)	(Ge)	23.98±0.7 0.78±0.7	0.24±0.4 98.78±0.2	75.78±0.2 0.44±0.4	5.6523±0.0006
2.	36.75 Bi 16.77 Ge 46.48 Sn	L (Ge)	(Ge)	24.91±0.6 0.42±0.8	1.92±0.3 98.21±0.1	73.17±0.8 1.37±0.5	5.6568±0.0001
3.	16.29 Bi 60.83 Ge 22.88 Sn	L (Ge)	(Ge)	38.63±0.2 0.28±0.4	1.52±0.3 99.07±0.7	59.85±0.1 0.65±0.9	5.6561±0.0007
4.	60.18 Bi 23.01 Ge 16.81 Sn	L (Ge)	(Ge)	41.87±0.3 0.82±0.1	0.24±0.6 98.91±0.7	57.89±0.3 0.27±0.2	5.6569±0.0002
5.	53.36 Bi 23.30 Ge 23.34 Sn	L (Ge)	(Ge)	21.13±0.3 0.47±0.8	0.62±0.2 99.11±0.4	78.25±0.9 0.42±0.5	5.6530±0.0006

Detected phases are L and (Ge) solid solution. (Ge) solid solution is rich with germanium and can dissolve neglected amount of tin and bismuth. EDS result shows that L phase have different composition depending on composition of the samples. In general L phase is rich in tin and bismuth and dissolves a negligible amount of germanium.

SEM micrographs of the sample 2 annealed at 300 ºC present at Figure 3.

.

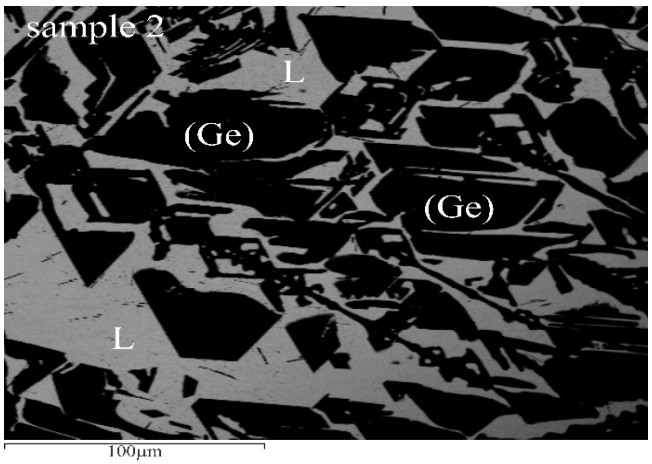

Figure 3: SEM micrographs of the sample 2 annealed at 300 ºC

From microstructure it is visible that (Ge) solid solution appears as a dark phase and L phase a gray phase.

The EDS results obtained for the samples annealed at 300 °C are given in Table 3 and compared with the calculated isothermal section at 300 °C. Figure 4 presents comparison of the calculated phase diagram and the EDS results.

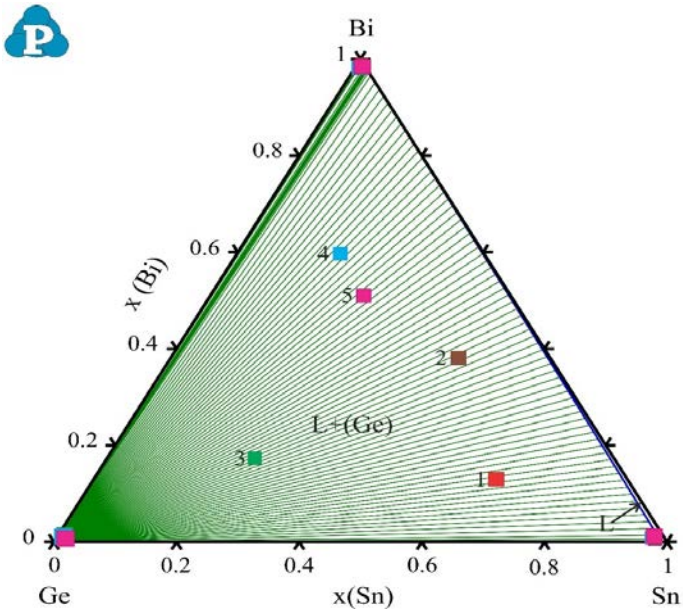

Figure 4: Calculated isothermal section at 300 °C compared with EDS results given in Table 3

The calculated isothermal cross section at 300° C consists of two phase regions. One is a single-phase region L, and the other is a two-phase region L+(Ge). By comparing the EDS composition of the tested samples, it is determined that all samples are from the two-phase L+(Ge) region, the same region as the experimentally detected samples. The EDS phase compositions agree well with the calculated phase compositions.

3.3. Microstructural analysis of slowly-cooled samples

Twelve slowly cooled ternary samples, marked with numbers from 1 to 12, were subjected to the tests of mechanical and electrical properties. Overall compositions of samples were situated along three vertical sections (samples 1 to 4, along Bi-GeSn vertical section, samples 5 to 8 along Ge-BiSn vertical section and samples from 9 to 12 along Sn-BiGe vertical section). Figure 5 presents calculated isothermal section at 25 ºC with marked nominal composition of tested ternary alloys.

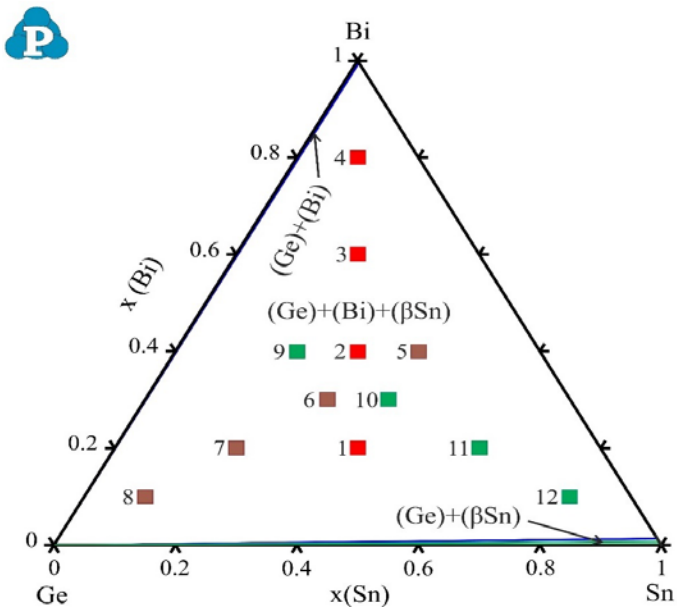

Figure 5: Predicted isothermal section at 25 ºC with marked compositions of tested alloys

Before determination of hardness and electrical conductivity samples were analyzed using XRD and their microstructure was observed with light optical microscopy. Results of XRD analysis of all samples revealed that all samples have (Ge), (Bi) and (βSn) phases in microstructure. Three microstructures of samples 1, 4 and 7 are given in Figure 6.

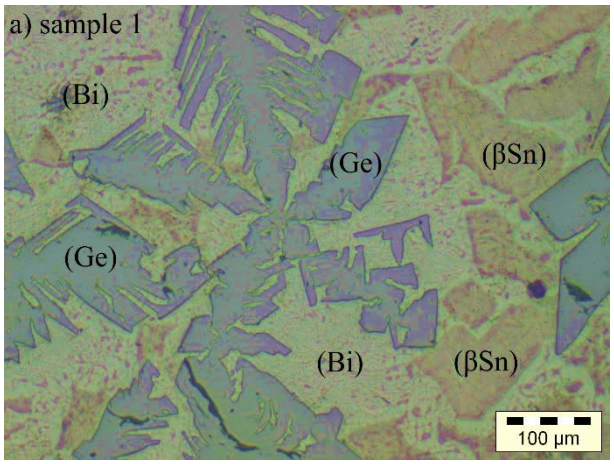

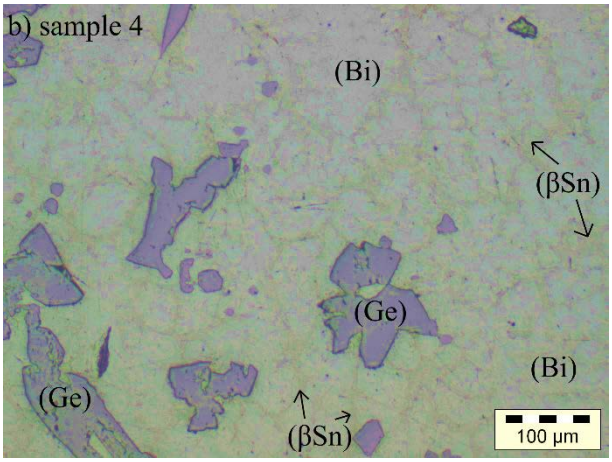

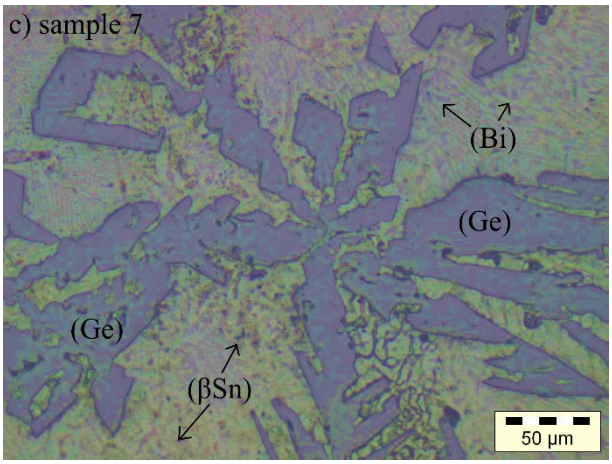

Figure 6: LOM micrographs of a) sample 1, b) sample 4 and c) sample 7

Phases which appear in microstructures are marked at presented micrographs.

3.3.1. Brinell hardness measurements

Twelve ternary samples and three binary samples were subjected to the Brinell hardness measurements. Based on repeated measurements, mean values of Brinell hardness were calculated and presented in Table 4. Literature values of hardness for pure elements [12] are also shown in Table 4 for comparison.

Table 4: Compositions of the investigated samples at room temperature and related Brinell hardness values

N.	Alloy nominal composition (at. %)			Measured value (MN/m^2)			Mean value (MN/m^2)
	x(Bi)	x(Ge)	x(Sn)	1	2	3	
B1	**0**	0.5	0.5	19.40	24.20	18.60	20.73
1	**0.2**	0.4	0.4	27.80	28.00	28.30	28.03
2	**0.4**	0.3	0.3	23.90	26.20	24.80	24.96
3	**0.6**	0.2	0.2	22.60	22.00	24.40	23.00
4	**0.8**	0.1	0.1	23.60	19.10	20.20	20.96
Bi	**1**	0	0				94.20 [12]
B2	0.5	**0**	0.5	15.40	12.30	16.20	14.63
5	0.4	**0.2**	0.4	31.90	32.70	32.30	32.30
6	0.3	**0.4**	0.3	38.80	43.10	42.80	41.56
7	0.2	**0.6**	0.2	41.60	46.20	44.80	44.20
8	0.1	**0.8**	0.1	63.30	58.50	56.20	59.33
Ge	0	**1**	0				973.40 [12]
B3	0.5	0.5	**0**	213.20	215.60	217.40	215.40
9	0.4	0.4	**0.2**	37.30	38.00	39.00	38.10
10	0.3	0.3	**0.4**	35.50	36.80	34.90	35.73
11	0.2	0.2	**0.6**	43.40	42.10	42.80	42.76
12	0.1	0.1	**0.8**	39.90	42.30	41.20	41.13
Sn	0	0	**1**				51.00 [12]

In addition to the tabular presentation, the obtained values for hardness are also presented graphically. Figure 7 shows a graphical representation of the relationship between the hardness of the tested alloys and the composition of the alloys.

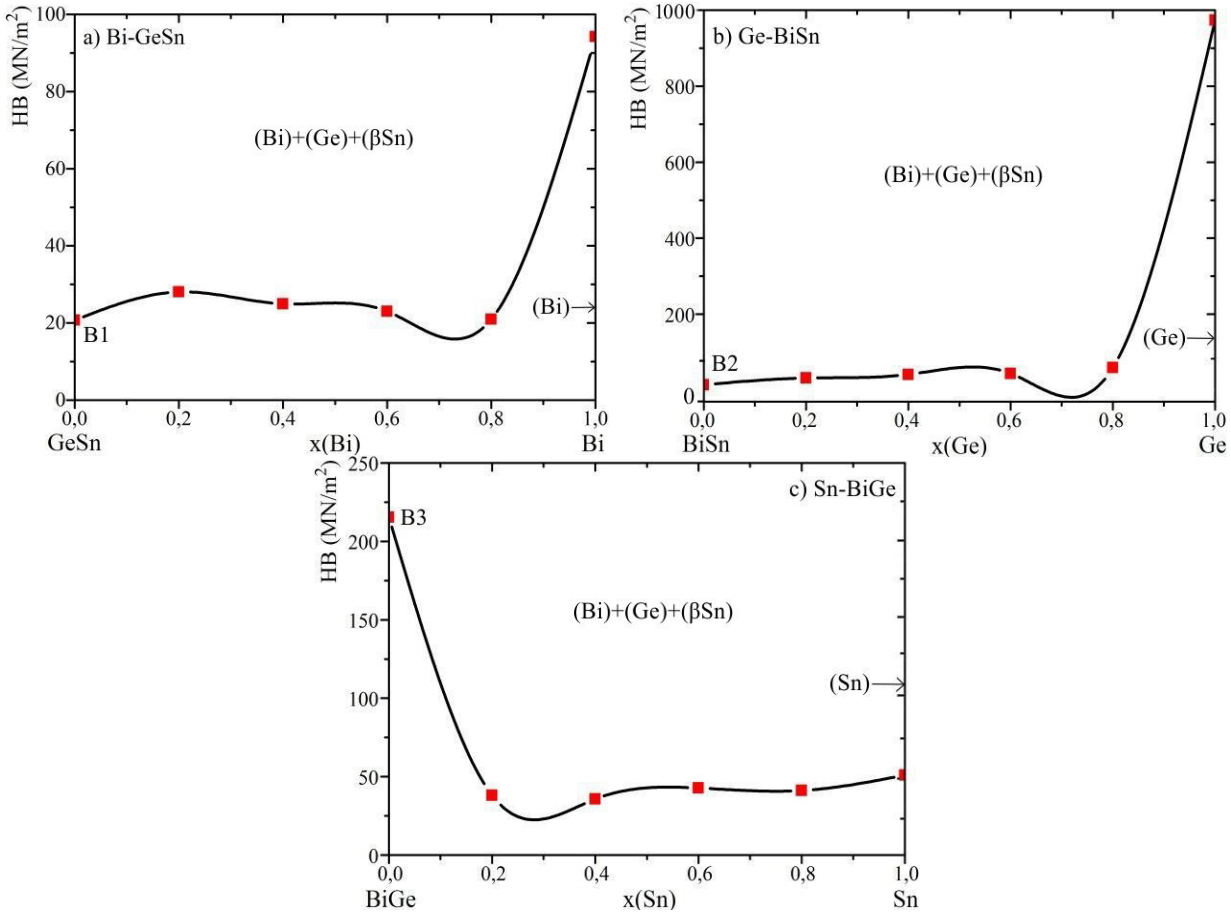

Figure 7: Graphical presentation of Brinell hardness dependence of composition and phase fraction: a) vertical section Bi-GeSn, b) vertical section Ge-BiSn and c) vertical section Sn-BiGe

The highest value of hardness for ternary alloys was measured on the sample Bi10Ge80Sn10 of 59.33 MN/m2, which is understandable due to the high amount of germanium.

As none of the S-models (Scheffe-model) met the adequacy requirements, the so-called SV-models (Slack-Variable mixture models) were used [13,14]. The Quartic Slack Mixture model was selected. By utilizing experimentally determined values of hardness given in

Table 5 mathematical model of the dependence of the Brinell hardness on composition for the Bi-Ge-Sn alloys was developed. The diagnosis of the statistical properties of the assumed model found that the distribution of residuals is not normal and that it is necessary to transform the mathematical model in order to meet the conditions of normality. The Box-Cox diagnostics recommends the ”Inverse Square Root“ transformation for the variance stabilization.

The final equation of the predictive model in terms of Real components is:

$$1/Sqrt(HB)=0.0317625+0.07459893\cdot(Bi)+1.39074537\cdot(Sn)-3.14882\cdot(Bi)\cdot(Sn) -0.0033572\cdot(Bi2)-2.7651581\cdot(Sn2)+4.02037782\cdot(Bi2)\cdot(Sn)+3.92451675\cdot(Bi)\cdot(Sn2) +1.48355978\cdot(Sn3) -3.2914706\cdot(Bi2)\cdot(Sn2) \quad (1)$$

The repeated analysis for Inverse Square Root model transformation confirms the significance of the Transformed Quartic Slack Mixture model. In this case, ANOVA confirms the adequacy of the Reduced Quartic Slack Mixture model (Table 5).

Table 5: ANOVA for Reduced Quartic Slack Mixture model

Source	Sum of Squares	df	Mean Square	F Value	p-value Prob > F
Model	0.05065	9	0.00563	35.49194	0.00002
A-Bi	0.00022	1	0.00022	1.40959	0.26918
C-Sn	0.00593	1	0.00593	37.37938	0.00029
AC	0.00362	1	0.00362	22.82148	0.00140
A^2	0.00000	1	0.00000	0.00310	0.95699
C^2	0.00286	1	0.00286	18.04155	0.00281
A^2C	0.00597	1	0.00597	37.62949	0.00028
AC^2	0.00175	1	0.00175	11.06407	0.01044
C^3	0.00185	1	0.00185	11.65229	0.00917
A^2C^2	0.00118	1	0.00118	7.44329	0.02592
Residual	0.00127	8	0.00016		
Cor Total	0.05191	17			

The F-value of the Model is 35,49 and it implies that the model is significant. In this case, all model terms are significant. R-squared and other statistics after the ANOVA have appropriate values which confirm the justification of the choice of the adopted mathematical model (Table 6).

Table 6: R-squared and other statistics after the ANOVA

Std. Dev.	0.01259	R-Squared	0.97557
Mean	0.16054	Adj R-Squared	0.94808
C.V. %	7.84322	Pred R-Squared	0.78256
PRESS	0.01129	Adeq Precision	24.09909

The diagnosis of the statistical properties of the assumed model found that the distribution of residuals are normal. After the applied Box-Cox procedure, the value of λ is -0.5, the optimum value of λ is -0.26 and the 95% confidence interval for λ (Low C.I.=-0.79, High C.I.=0.11) contains the value -0.5, thus proving the justification of the model transformation (Figure 8).

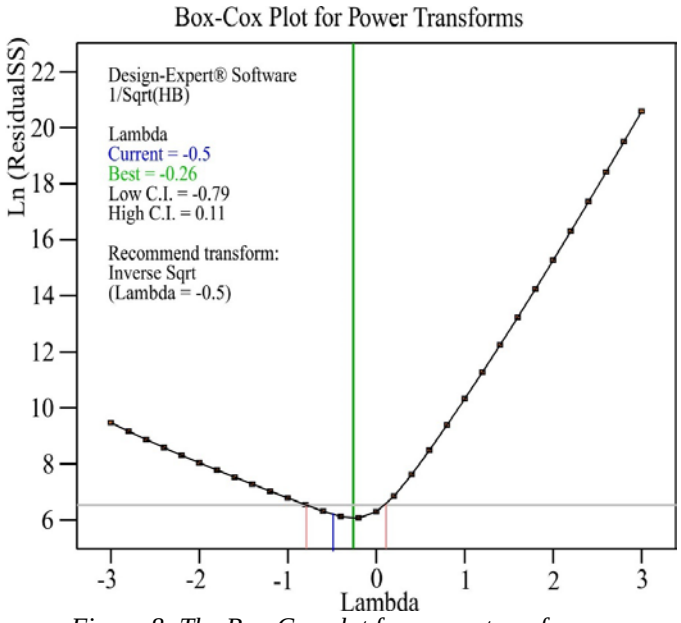

Figure 8: The Box-Cox plot for power transforms

Iso-lines contour plot for Brinell hardness of alloys defined by equation 1 is shown in Figure 9.

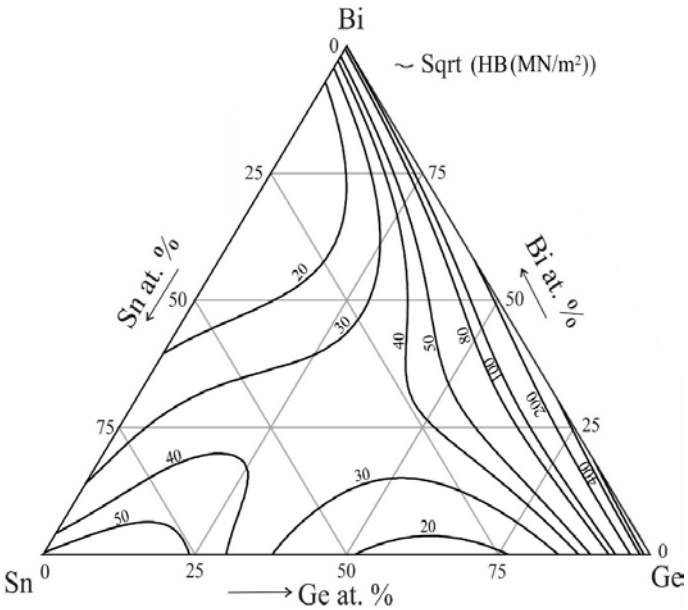

Figure 9: Calculated iso-lines of Brinell hardness in ternary Bi-Ge-Sn system with R2 =0.976

3.3.2. Electrical conductivity measurements

Measurements of electrical conductivity were performed on the same group of samples used for hardness test. For all investigated samples electrical conductivity measurements were repeated four times at different positions and obtained values for each measured point are given in Table 7. Beside measured values, Table 7 also includes calculated mean values and literature values of electrical conductivity for pure elements [15].

Table 7: Compositions of the investigated samples at room temperature and related electrical conductivity values

N.	Alloy nominal composition (at. %)			Value (MS /m)				Mean value
	x(Bi)	x(Ge)	x(Sn)	1	2	3	4	(MS/m)
B1	**0**	0.5	0.5	2.8010	2.7370	2.7800	2.7680	2.7710
1	**0.2**	0.4	0.4	0.5323	0.7698	0.6397	0.7885	0.6825
2	**0.4**	0.3	0.3	0.4978	0.4757	0.5042	0.4989	0.4941
3	**0.6**	0.2	0.2	0.8899	0.6365	0.7895	0.6325	0.7371
4	**0.8**	0.1	0.1	0.9636	0.9800	0.9993	0.8998	0.9606
Bi	**1**	0	0					0.77 [15]
B2	0.5	**0**	0.5	1.3699	1.0236	1.3698	1.0233	1.1966
5	0.4	**0.2**	0.4	0.8161	0.8317	0.8561	0.8383	0.8355

6	0.3	**0.4**	0.3	0.7896	0.6356	0.7853	0.6669	0.7193
7	0.2	**0.6**	0.2	0.3168	0.3156	0.3147	0.3158	0.3157
8	0.1	**0.8**	0.1	0.3695	0.2225	0.2314	0.2323	0.2639
Ge	0	**1**	0					0.002 [15]
B3	0.5	0.5	**0**	0.3430	0.3410	0.3530	0.3440	0.3452
8	0.4	0.4	**0.2**	0.3080	0.3068	0.3091	0.3087	0.3081
10	0.3	0.3	**0.4**	0.3889	0.4545	0.5232	0.4999	0.4666
11	0.2	0.2	**0.6**	2.0450	1.9999	2.0050	2.0254	2.0188
12	0.1	0.1	**0.8**	3.1232	3.1252	2.9362	2.9316	3.0290
Sn	0	0	**1**					9.1 [15]

Figure 10 presents graphical presentation of results (mean value) given in Table 7 for easier overview of the results.

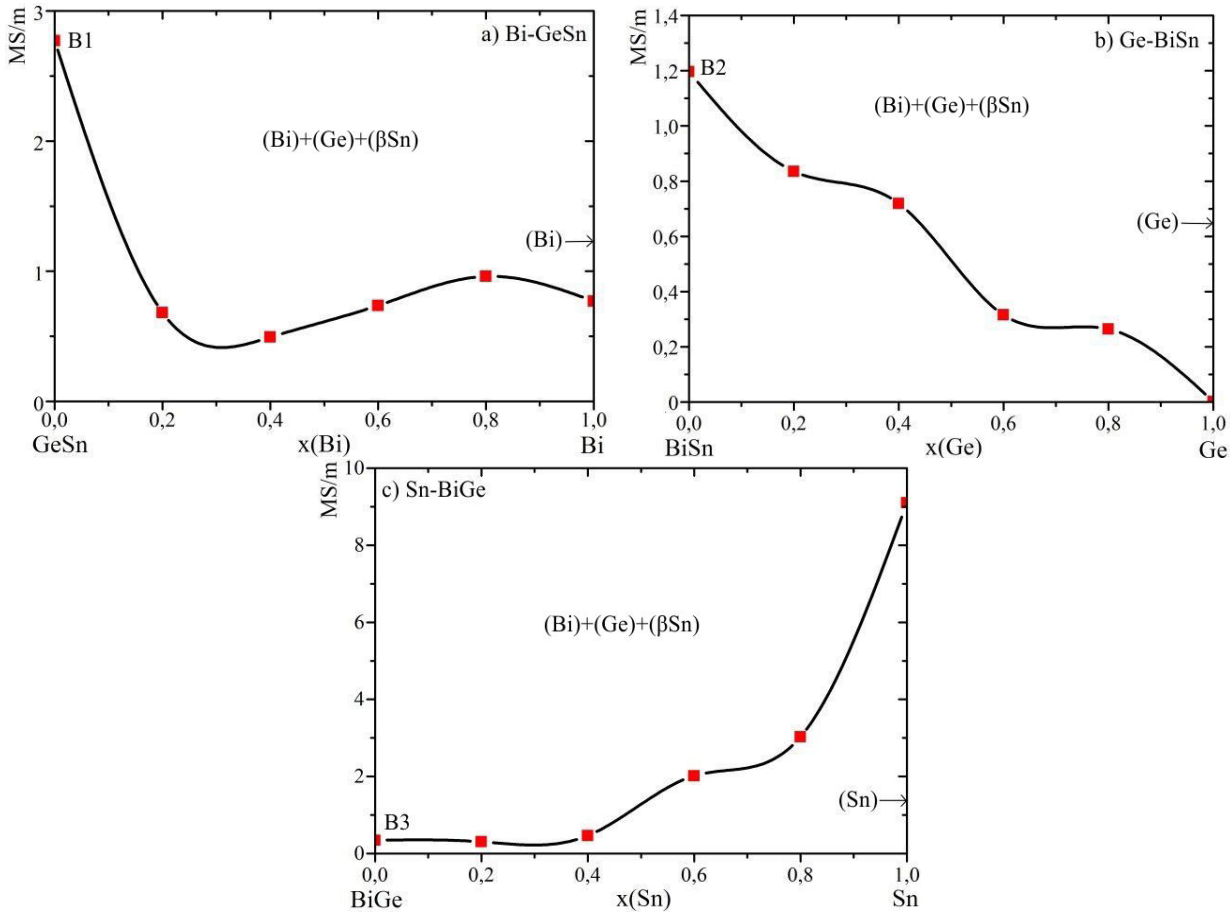

Figure 10: Graphical presentation of electrical conductivity dependence of composition and phase fraction a) vertical section Bi-GeSn, b) vertical section Ge-BiSn and c) vertical section Sn-BiGe

According to the obtained results, the triple alloy Bi10Ge10Sn80 has the highest value of electrical conductivity, 3.0290 MS/m, which is expected because in this combination of bismuth, germanium and tin, tin has the highest electrical conductivity compared to the other two components.

Special Quartic Mixture model was suggested as a final equation for prediction of electrical conductivity. The diagnosis of the statistical properties of the assumed model found that the distribution of residuals is not normal and that it is necessary to transform the mathematical model in order to meet the conditions of normality. The Box-Cox diagnostics recommend the ”Square Root“ transformation for the variance stabilization.

The final equation of the predictive model in terms of Actual components is:

$$\text{Sqrt}(\sigma)=0.976127\cdot(\text{Bi})+0.0501598\cdot(\text{Ge})+2.8830787\cdot(\text{Sn})+0.4271847\cdot(\text{Bi})\cdot(\text{Ge}) -3.0859792\cdot(\text{Bi})\cdot(\text{Sn})+0.514126\cdot(\text{Ge})\cdot(\text{Sn})-26.711332\cdot(\text{Bi})\cdot(\text{Ge})\cdot(\text{Sn2}) \quad (2)$$

The repeated analysis for Square Root model transformation confirms the significance of the Transformed Special Quartic Mixture model. In this case, ANOVA confirms the adequacy of the Special Quartic Mixture model (Table 8).

Table 8: ANOVA for Special Quartic Mixture model

Source	Sum of Squares	df	Mean Square	F Value	p-value Prob > F
Model	6.97359	6	1.16227	48.75690	0.00000027
Linear Mixture	5.68286	2	2.84143	119.19764	0.00000004
AB	0.00972	1	0.00972	0.40762	0.53624788
AC	0.43643	1	0.43643	18.30800	0.00130137
BC	0.01211	1	0.01211	0.50815	0.49078544
ABC^2	0.18397	1	0.18397	7.71754	0.01796658
Residual	0.26222	11	0.02384		
Cor Total	7.23581	17			

The F-value of the Model is 48.76 and it implies that the model is significant. R-squared and other statistics after the ANOVA have good values which confirm the justification of the choice of the adopted mathematical model (Table 9).

Table 9: R-squared and other statistics after the ANOVA

Std. Dev.	0.15440	R-Squared	0.96376
Mean	0.99388	Adj R-Squared	0.94399
C.V. %	15.53469	Pred R-Squared	0.81299
PRESS	1.35317	Adeq Precision	29.42299

The diagnosis of the statistical properties of the assumed model found that the distribution of residuals are normal. After the applied Box-Cox procedure, the value of λ is 0.5, the optimum value of λ is 0.32 and the 95% confidence interval for λ (Low C.I.=0.10, High C.I.=0.55) contains the value 0.5, thus proving the justification of the model transformation (Figure 11).

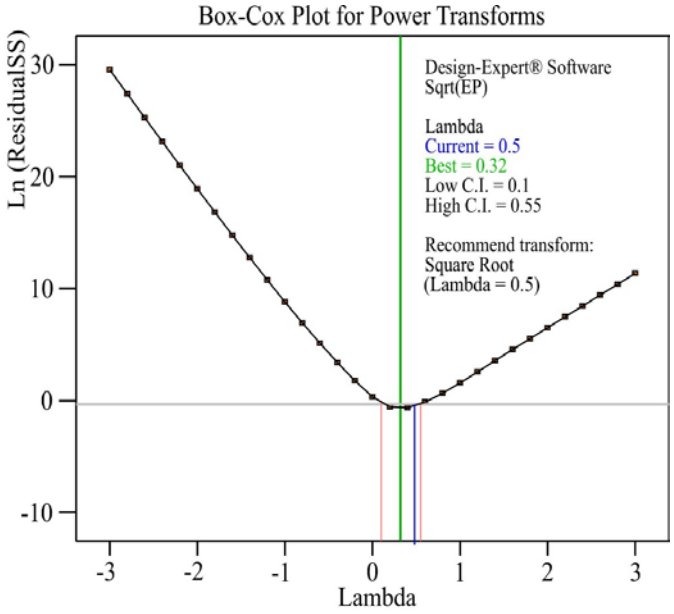

Figure 11: The Box-Cox plot for power transforms

Iso-lines contour plot for Electrical conductivity of Bi-Ge-Sn alloys defined by equation 2 is shown in Figure 12.

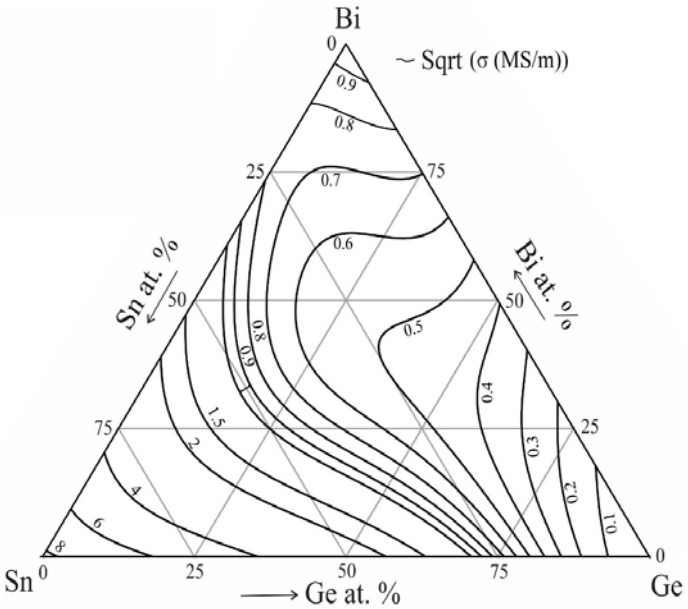

Figure 12: Calculated iso-lines of Electrical conductivity in ternary Bi-Ge-Sn system with R2 =0.964

4. CONCLUSION

In this study, for ternary Bi-Ge-Sn system are experimentally investigated three isothermal sections at 200, 300 and 25 °C. SEM-EDS and XRD analysis were applied for analysis of the chosen ternary samples after long-term annealing. Experimental results SEM-EDS and XRD techniques were compared with calculated phase diagrams at 200 and 300 °C and good agreement between data is reached. By using thermodynamic data set, isothermal section at 25 °C was calculated and three different phase fields were predicted. One of three phase region were confirmed with EDS and XRD results. On twelve ternary alloys and three binary alloys were performed tests microstructural, hardness and electrical conductivity. With SEM and LOM microstructures of tested alloys were observed. On 25 °C detected phases with XRD method are (Ge), (Bi) and (βSn) solid solutions. All results from Brinell hardness test and electrical conductivity were used for predicting a mathematical model for calculation of properties along all composition range.

ACKNOWLEDGEMENTS

This work has been supported by the National Nature Science Foundation of China (project No.51950410600) and the Ministry of Education, Science and Technological Development of the Republic of Serbia (Grant No. OI172037).

REFERENCES

[1] Premovic, M., Minić, D., Kolarevic, M., Manasijevic, D., Živković, D., Djordjevic, A., Milisavljevic, D., 2017. Rev Metal. 53(3), p. e098
[2] Premović, M., Manasijević, D., Minić, D., Živković, D., 2016. Kovové Mater. 54(1), p. 45
[3] Premovic, M., Du, Y., Minic, D., Zhang, C., Manasijevic, D., Balanovic, Lj., Markovic, I., 2017. J. Alloy Compd. 726, p. 820
[4] Djordjević A., Minić D., Premović M., Manasijević D., Ćosović V., JPED, 2019, 40(4), p 623-637
[5] Lacaita, A.L., Wouters, D.J., 2008. Phys. Status Solidi A Appl. Mater., 205, p. 2281
[6] Ou, S. L., Cheng, C. P., Yeh, C. Y., Chung, C .J., Kao, K. S., Lin, R. C., 2011. Adv. Mater. Res., 189, p. 4430
[7] Ielmini D., Lacaita, A. L., 2011. Mater. Today, 14(12), p. 600
[8] Nemec, P., Nazabal, V., Moreac, A., Gutwirth, J., Benes, L., Frumar, M., 2012. Mater. Chem. Phys., 136, p. 935
[9] Chevalier P.-Y., Thermochim. Acta, 1988, 132, p. 111–116
[10] Vizdal J., Braga M. H., Kroupa A, Richter K. W., Soares D., Malheiros L. F., Ferreira J., Calphad, 2007, 31, p. 438–448
[11] Feutelais Y, Legendre B, and Fries S.G., Calphad, 1996, 20(1), p. 109-123
[12]http://periodictable.com/Properties/A/BrinellHardness.al.html, access 29.11.2018
[13] Cruz-Salgado Javier, Selecting the Slack Variable in Mixture Experiment, Ingeniería Investigación y Tecnología, 2015, 14 (4), p 613-623
[14] G. F. Piepel, D. C. Hoffmann, S. K. Cooley, Slack-Variable versus Mixture Modeling for Mixture Experiments: A Definitive Comparison, 2018.
[15]http://periodictable.com/Properties/A/ElectricalConductivity.an.html, access 25.12.2018